JCHR (2023) 13(4), 739-746

Journal of Chemical Health Risks

jchr.damghan.iau.ir

ORIGINAL ARTICLE

Measurement of Effective Dose to Head and Neck Critical Organs in Computed Tomography

Amir Hosein Goodarzi[1], Mastaneh Sanei[*2], Hadi Hasanzadeh[3], Zohreh Khosravi[1], Ahmad Bitarafan-Rajabi[4], Alireza Emadi[5]

[1] *Department of Radiation Oncology, Iran Gamma Knife Center, Tehran, Iran*

[2]*Department of Radiation Oncology, Haft-e-Tir Hospital, Iran University of Medical Sciences, Tehran, Iran*

[3]*Department of Radiation Oncology, Pardis Noor Niloo Medical Imaging and Cancer Center, Tehran, Iran*

[4]*Cardiovascular Interventional Research Center, Department of Nuclear Medicine, Rajaie Cardiovascular Medical and Research Center, Iran University of Medical Sciences, Tehran, Iran*

[5]*Deputy of Research and Technology, Semnan University of Medical Sciences, Semnan, Iran*

(Received: 19 November 2021 Accepted: 10 April 2022)

KEYWORDS

Computed tomography scan;
Film dosimetry;
Phantoms;
Carcinogenesis

ABSTRACT: One of the most effective methods to report organ dose in CT scan (Computed Tomography scan) is to report effective dose. This study aimed to investigate the actual dose during head and neck CT scans using an anthropomorphic head phantom. In this study, an anthropomorphic phantom was constructed with natural bone and paraffin wax. Then, we considered several sites in the phantom to investigate the dose. These sites include the Brain, Thyroid, Parotid, and Lens, which were filled by Gafchromic films. Finally, we irradiated the phantom using several CT protocols. Our findings indicate that the dose of the considered organs was in the different ranges according to the protocol used. The highest dose range was related to the ten-slice spiral, ranging from 0.75 to 15.8 mGy (Mean). We showed the lowest dose range in SPECT-CT which was in the range of 0.55 to 0.1 mGy (Mean). The absorbed dose of the eyes was much higher in most protocols compared to the other organs. There is also the most significant difference between the lens and the other organs in the ten-slice spiral CT. Comparing the 10 and 256 slice scanners; we showed that the organ dose in the 256 slice is less than ten slices. The lowest mean organ dose (mGy) and SD (Standard Deviation) are related to the SPECT CT, which are 0.76±0.03, 0.95±0.02, 0.78±0.02, and 0.71±0.02 for the brain, parotid, lens, and thyroid, respectively.

INTRODUCTION

Computed Tomography (CT) is one of the most valued imaging techniques that use ionizing radiation and produces sectional images of the patient body for early diagnosis of diseases [1-4]. With the worldwide improvement of CT technology and utilizing multislice CT scanners, an increase in the demand for CT examinations has been followed [5,6]. Although CT scan is recognized as a high dose procedure, it is one of the most widely considered technologies in medicine due to its high-quality images and better diagnosis of diseases [7-9]. So, CT is utilized for a wide range of applications, including diagnosis of injuries, infections, tumors, and other disorders, which necessitate estimation of absorbed dose to organ at risk [6, 10].

As the potential risks of ionizing radiation used in CT scan, there would be a necessity to compromise the advantages of CT scan against the potential risk of cancer induction due to its relatively high dose of

*Corresponding author: sanei.m@iums.ac.ir (M. Sanei)
DOI: 10.22034/jchr.2022.1945293.1457

radiation compared to other diagnostic modalities [3, 5]. Regarding increasing number of CT scans, the patient dose has become a significant concern because of its portion of the population dose [10-12]. Different methods exist to measure CT doses, such as CT Dose Index (CTDI), Dose Length Product (DLP), and effective organ dose. CTDI is one of the most frequently used parameters to estimate radiation exposure in CT scans [6, 13]. Most studies report their findings based on CTDI to measure organ radiation absorbed dose [14]. The effective organ dose could be measured by TLDs or Gafchromic films, which placed in the targeted organs in an anthropomorphic phantom to examine the radiation absorbed dose. This parameter is a measure of organ dose to present an estimation of radiation carcinogenesis due to stochastic effects [15, 16].

So, this method can be applied for organ dosimetry in different protocols to facilitate dose optimization, and has been shown that practical organ dosimetry is a standard method to measure radiation risks [17, 18].

Absorbed dose to critical organs has been investigated previously using anthropomorphic head phantom, and it has been concluded that the mean absorbed dose to brain, eyes, and thyroid during head computed tomography imaging is firmly lower than the ICRP recommendation [19].

Although CT scan procedures have a higher effective dose compared to other imaging techniques, it is the most established practice; therefore, more attention should be paid to this imaging protocol [5, 20].

The main goal of this study is to focus on evaluating absorbed dose in most common CT protocols such as Angio, Spiral, Sequential, Flash, and Dual Source with several CT machines. An anthropomorphic head phantom was implemented to measure the absorbed dose during the CT exam using Gafchromic films.

MATERIALS AND METHODS

Phantom

An anthropomorphic head phantom was produced using a human skull and paraffin wax with NaCl as an impurity, respectively [6]. To estimate total brain dose, we divided the brain into three regions, including Upper Brain, Mid Brain, and Brain Stem from the skull apex downwards and the anatomical position of the left to right parotid on the base of the skull (Figure 1). We also considered the weight coefficients of 0.25, 0.5, and 0.25 for area, respectively. Besides, two small applicators with film insertions were considered at the side lobes of the thyroid to measure thyroid dose. Absorbed dose to the lens of the eye was measured at the surface.

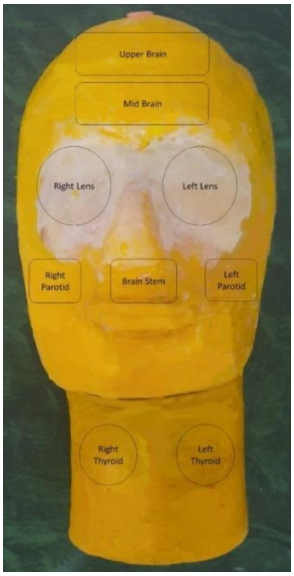

Figure 1. Head & neck phantom with the approximate position of considered organs.

Calibration of Dosimeters

To obtain a calibration curve, multiple pieces of films were divided into several groups, each consisting three pieces, receiving a known dose which was measured using a dose monitor device (Pehamed, Germany). To

obtain the calibration equation, the net optical density (netOD (Net Optical Density)) was obtained from the following relationship after reading with a flatbed scanner:

$$netOD=OD_{exp}-OD_{unexp}=\log_{10}[(PV_{nexp}-PV_{bg})/(PV_{exp}-PV_{bg})]$$

PV_{unexp} is the pixel value of the unexposed film, PV_{exp} is for the exposed film, and PV_{bg} is for opaque black cardboard.

Imaging Protocols

As shown in Figure 2, we used several CT machines, including two SPECT-CT as Siemens Symbia Truepoint, and GE Infinia Hawkeye 4 and two CT machines, including Siemens Somatom definition flash 256 slices and Somatom Sensation 10 slice. The most common imaging protocols as spiral, sequential, flash, dual-source and CT Angio for an adult man for the head region were selected to simulate the exact condition related to phantom measurement; no parameters of the scan were changed. The scan parameters are shown in Table 1.

Dosimetric Measurements

Our target organs for which the doses were measured included the whole brain (with an estimation of measured doses from two perpendicular applicators), the lens of the eye, thyroid, and parotid. The exposed films were scanned as previously described, and the red channel from the RGB image was extracted in Matlab (R2021a, Mathworks, USA) to obtain the organ dose. To increase reproducibility and reduce noise, each measurement triplicates.

Table 1. The scan parameters related to the protocols used in this study.

Protocol	kV/ mAs
SPECT CT (1)	80/ 225
SPECT CT (2)	130/ 260
SPECT CT GE	140/ 100
256 Slice CT Angio	120/ 175
256 Slice Dual Source	80, 140/ 222
256 Slice Flash	120/ 160
256 Slice Sequential	120/ 340
256 Slice Spiral	120/ 390
10 Slice Brain Angio	120/ 95
10 Slice Sequential	120/ 300
10 Slice Spiral (1)	80/ 320
10 Slice Spiral (2)	120/ 320

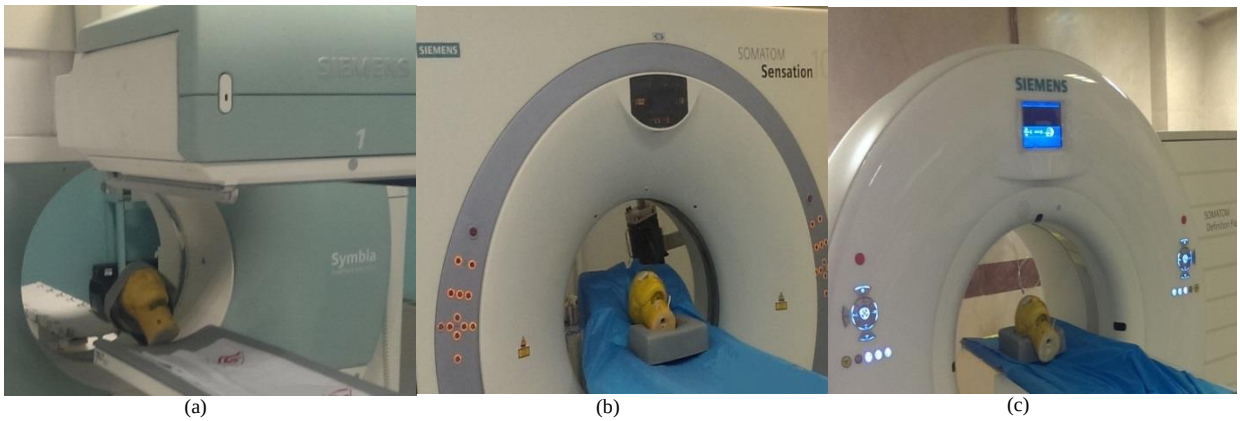

(a) (b) (c)

Figure 2. The head phantom was placed at the (a) SPECT-CT, (b) 10 slice CT and (c) 256 slice.

RESULTS

Figures 3 to 6 show data that are related to the calibration of Gafchromic films used in this study. The calibration was performed in different kVs, including 80, 120, 130, and 140kV. We calculated the Calibration Equation and Correlation Coefficient (R^2) in each kV. In the calibration equation, y (the vertical axis) represents the dose in mGy, and x (the horizontal axis) shows the netOD.

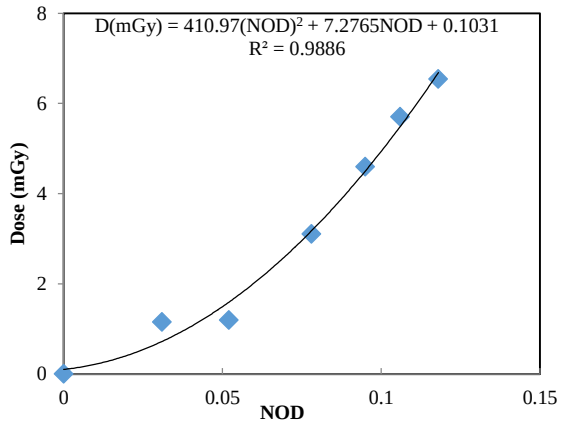

Figure 3. Calibration curve at 80kV.

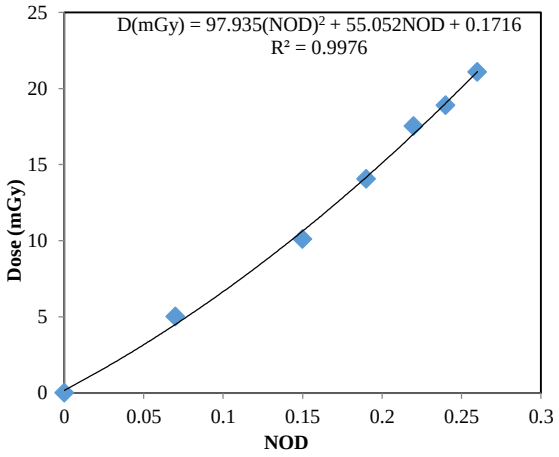

Figure 4. Calibration curve at 120kV.

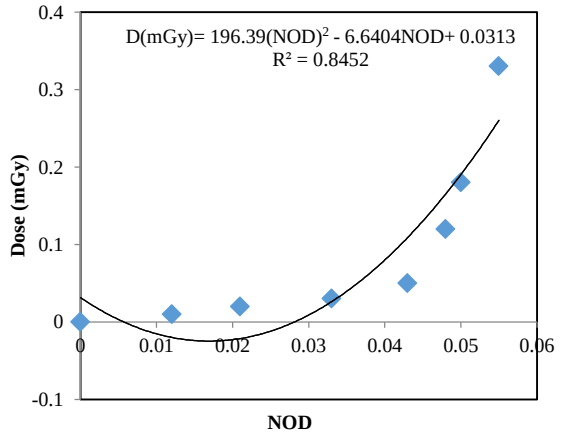

Figure 5. Calibration curve at 130kV

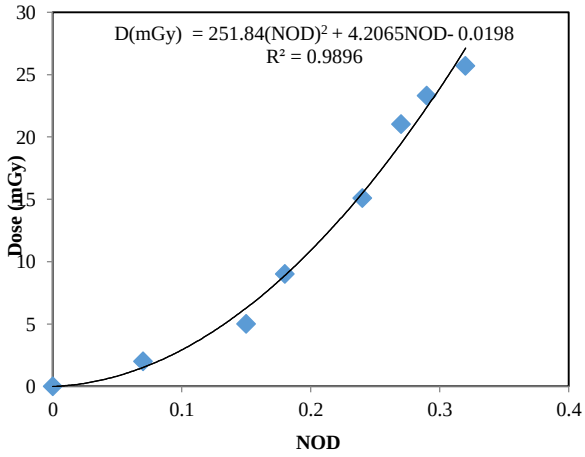

Figure 6. Calibration curve at 140kV.

Figure 7 presents the mean absorbed dose to the critical organs, including the Brain, Thyroid, Parotid, and lens of the eye. The absorbed dose to the brain, Thyroid, and Parotid is an indicator of the mean depth dose, and the dose delivered to the lens is described as the mean surface dose.

According to Figure 7, the highest dose delivered to the brain has been observed in protocol 10 Slice Spiral (120kV, 320mAs), while the lowest absorbed dose is related to the protocol SPECT-CT GE (140kV, 100mAs). According to the results in Figure 7, the highest absorbed dose to the thyroid is shown in the protocol SPECT-CT (80kV, 225mAs), and the lowest dose is related to protocol 256 slice Dual Source (80/140kV. 222mAs).

As shown in Figure 7, the highest absorbed dose to parotid is as same as thyroid, but the lowest dose has been observed in protocol 256 Slice Dual Source. Figure 7 also shows that the highest dose delivered to the lens is related to protocol 10 Slice Spiral (120kV, 320mAs), and the lowest dose has been observed in protocol SPECT-CT GE, precisely the same as the brain.

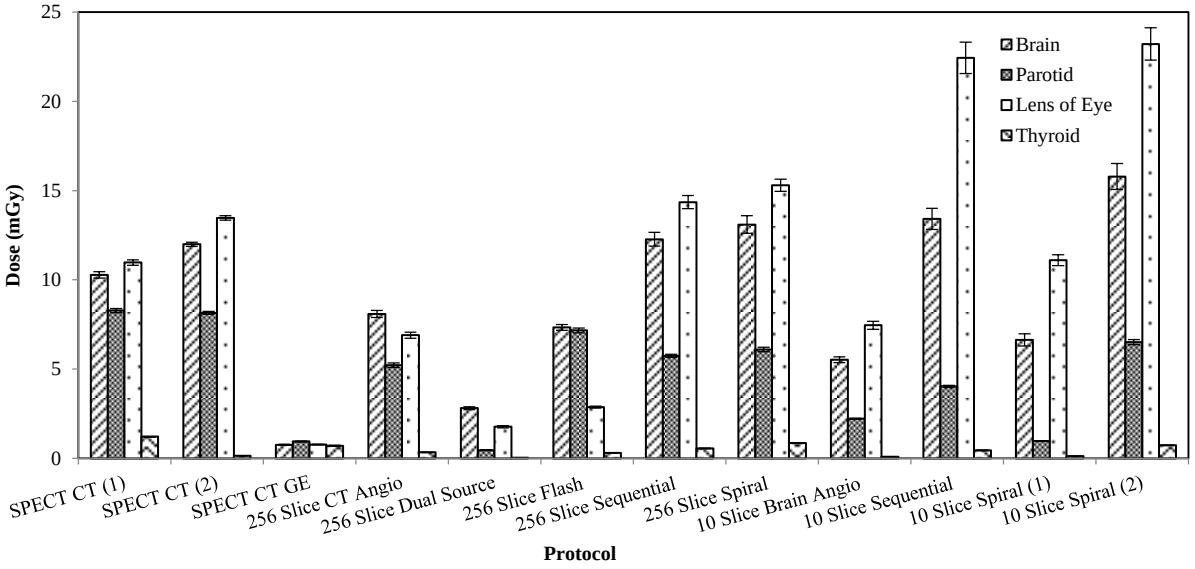

Figure 7. Mean organ dose (SD) in mGy in different protocols.

DISCUSSION

In the present study, we compared doses to the Brain, Parotid, Thyroid, and lens of the eye in several CT scanners under clinical conditions. To simulate a more accurate clinical condition, we used an anthropomorphic phantom in this study that provided appropriate tissue organs. Gafchromic films, which are sensitive to low doses of radiation embedded at related sites of the phantom to measure the organ dose.

Measurement of effective dose is a well-known method used to analyze radiation risk and is considered very valuable in calculating the dose received by the patient. This method also allows us to compare different CT protocols so that a lower dose reaches the patient during the CT examination [19, 21].

The patient radiation absorbed dose from CT procedures, is influenced by several factors such as beam quality (kVp), slice thickness, the current tube time (mAs), and the number of detectors in the scanner. There is considerable evidence suggesting that the effective organ dose delivered by CT procedures can be directly related to the increase in cancer incidence [4].

In the present study, we compared the organ dose in several CT protocols, which are different in mAs, kVp, and the number of slices. The radiation dose of 10 Slice Spiral protocols (120kV, 320mAs) is much higher than the other protocols due to its high rate of CT parameters and the small number of slice scanners. However, we expect the organ dose should be lower in this protocol because it scans the body in a spiral path.

As is observed in Table 2, by comparing protocols SPECT-CT (80kV, 225mAs), SPECT-CT (130kV, 260mAs), and SPECT-CT GE (100kV, 140mAs), we showed that there is a relation between protocol dose and organ absorbed dose. According to the Table 1, in SPECT CT (130kV, 260 mAs) the doses which are delivered to the brain and lens of the eye are higher than the two other protocols due to the higher beam parameters. So with increasing the protocol dose, the organ dose also increases. In the case of the thyroid, the difference may be due to the strict collimation and its position relative to the slices [6]. This is precisely the case with the two other protocols, such as ten slice Spiral (80kV, 320mAs) and ten slice Spiral (120kV, 320mAs). As indicated in this Table and Figure 7, the lowest absorption dose is related to the SPECT-CT GE, which is significantly different from other protocols due to its shallow tube time-current product (mAs).

Table 2. Mean organ dose in mGy at three different CT protocols

Protocol	Brain/ mGy (Mean)	Parotid/ mGy (Mean)	Lens of Eye/ mGy (Mean)	Thyroid/ mGy (Mean)
SPECT-CT (80kV, 225mAs)	10.27	8.28	10.97	1.22
SPECT-CT (130kV, 260mAs)	11.99	8.15	13.46	0.14
SPECT-CT GE (140kV, 100mAs)	0.76	0.95	0.78	0.71

Our results showed the absorbed dose to the lens of the eye was the highest in almost all protocols, which could be due to exposure to primary radiation [22, 23]. The highest mean dose (mGy) and SD of the lens were 23.21± 0.9 in ten Slice Spiral (120kV, 320mAs).

Regarding the nature of CT angiography, which is tracing the blood flow in arteries, it requires the sectional images to be gathered fast, so it is better to use multidetector CT (MDCT) to take good images while reducing organ dose due to the higher number of detector arrays, like the 256-slice scanner [6]. However, according to our results, the absorbed dose in the 256-slice CT angiography protocol is a little more than the ten slice scanner because of the higher mAs used in the 256 slices CT Angio.

These results are consistent with the results reported by Seyedatashi et al., that compared the organ dose in ten slices and 256 slices CT Angio. They showed the absorbed dose in 256 slice is higher than ten slices [6].

It should be noted that in 256 Slice Dual Source and 256 Slice Flash protocols, due to the nature of the protocols and by utilizing tissue absorption coefficients at different voltages, we can achieve better images with lower doses, and as a result, lower organ doses are obtained as shown in our results.

As it can be seen from table 3, in sequential and spiral protocols with the difference in the slice numbers, the organ dose in 256 slice scanners (except for the thyroid in the Spiral protocol and thyroid and parotid in the Sequential protocol) is lower than ten slice scanners. There are several explanations that can be associated with lower doses of the 256 slices compared to ten slice protocols. It could be due to the higher number of detector arrays in 256 slice scanners, which causes a lower dose to reach the organs despite the higher CT parameters in the 256-slice protocol [6]. Our results are in agreement with the study conducted by Moore et al., who measured and compared radiation dose in 4-8 and 16 MDCT and showed that the radiation dose in 4-detector scanner is 47% higher than in 16-detector scanner, which correlates with our results [24].

The differences seen in the organs such as thyroid and parotid could be due to the direct incidence of CT exposure on dosimeter location in these organs.

Table 3. Mean organ dose in mGy at four different CT protocols.

Protocol	Brain/ mGy (Mean)	Parotid/ mGy (Mean)	Lens of Eye/ mGy (Mean)	Thyroid/ mGy (Mean)
10 Slice Spiral (120kV, 320mAs)	15.79	6.51	23.21	0.73
256 Slice Spiral (120kV, 390mAs)	13.1	6.1	15.3	0.87
10 Slice Sequential (120kV, 300mAs)	13.41	4.03	22.43	0.45
256 Slice Sequential (120kV, 340mAs)	12.27	5.74	14.35	0.56

CONCLUSIONS

A survey was performed on the most prevalent CT protocols to present data in hand in order to have an estimation of dose levels of such protocols, which helps health professionals to decide. It is concluded that if the dose delivered to the patient is high, the absorbed dose should be reduced by optimizing the dose using scan parameters modulation and technical measures [7] to make sure the patient and public dose do not cause cancer induction.

ACKNOWLEDGEMENTS

This work was made possible with the kind collaboration of the radiology department of Shahid Rajaei hospital, Haft e Tir hospital, and Shahid Chamran hospital.

Conflict of interests

The authors have no relevant financial or non-financial interests to disclose.

REFERENCES

1. Omar R., Hashim S., Ghoshal S., Shariff N., 2020. Dose assessment of 4-and 16-slice multi-detector computed tomography (MDCT) scanners. Radiation Physics and Chemistry. 168, 108445.

2. Hu S.Y, Hsieh M.S., Lin M-Y, Hsu C.Y., Lin T.C., How C.K., Wang C.Y., Che-Huang Tsai J., Wu Y.H., Chang Y.Z., 2016. Trends of CT utilisation in an emergency department in Taiwan: a 5-year retrospective study. BMJ open. 6(6), e010973.

3. De Gonzalez A.B., Salotti J.A., McHugh K., Little M.P., Harbron R.W., Lee C., Ntowe E., Braganza M.Z., Parker L., Rajaraman P., Stiller C., Stewart D.R., Craft A.W., Pearce M.S., 2016. Relationship between paediatric CT scans and subsequent risk of leukaemia and brain tumours: assessment of the impact of underlying conditions. British journal of cancer. 114(4), 388-94.

4. Alkhorayef M., Babikir E., Alrushoud A., Al-Mohammed H., Sulieman A., 2017. Patient radiation biological risk in computed tomography angiography procedure. Saudi journal of biological sciences. 24(2), 235-40.

5. Griglock T.M., Sinclair L., Mench A., Cormack B., Bidari S., Rill L., Arreola M., 2015. Determining organ doses from CT with Direct measurements in postmortem subjects: part 1—methodology and validation. Radiology. 277(2), 463-70.

6. Seyedatashi S.F., Athari M., Bitarafan-Rajabi A., Hasanzadeh H., Rafati M., Pouraliakbar H.R., Mohamadzadeh A., 2015. Dosimetric evaluation of multislice ct using anthropomorphichead phantom. Frontiers in Biomedical Technologies. 2(1), 31-35.

7. Al Ewaidat H., Zheng X., Khader Y., Abdelrahman M., Mustafa Alhasan M.K., Rawashdeh M.A., Dana Samir A.M., Khaled Zayed A.A., 2018. Assessment of radiation dose and image quality of multidetector computed tomography. Iranian Journal of Radiology. 15(3), e59554.

8. Smith-Bindman R., Lipson J., Marcus R., Kim K.P., Mahesh M., Gould R., Berrington de González A., L Miglioretti D., 2009. Radiation dose associated with common computed tomography examinations and the associated lifetime attributable risk of cancer. Archives of Internal Medicine. 169(22), 2078-86.

9. Sheppard J.P., Nguyen T., Alkhalid Y., Beckett J.S., Salamon N., Yang I., 2018. Risk of brain tumor induction from pediatric head CT procedures: a systematic literature review. Brain tumor research and treatment. 6(1), 1.

10. Santos F.S., Santana Pd.C., Alnso T.C., Mourão A.P., 2018. Dose variation with the use of eye bismuth shielding on head CT scans. Quarta Semana de Engenharia Nuclear e Ciências das Radiações. 31-36.

11. Akpochafor M.O., Adeneye S.O., Habeebu M.Y., Omojola A., Adedewe N., Adedokun A., Adewa D., Ajibade S.O., Ekpo V., Adebayo Aweda M., 2019. Organ Dose Measurement in Computed Tomography Using Thermoluminescence Dosimeter in Locally Developed Phantoms. Iranian Journal of Medical Physics. 16(2), 126-32.

12. Giansante L., Martins J.C., Nersissian D.Y., Kiers K.C., Kay F.U., Sawamura M.V., Lee C., M. M. S. Gebrim E., R. Costa P., 2019. Organ doses evaluation for chest computed tomography procedures with TL dosimeters: Comparison with Monte Carlo simulations.

Journal of Applied Clinical Medical Physics. 20(1), 308-20.

13. Kopp M., Loewe T., Wuest W., Brand M., Wetzl M., Nitsch W., Schmidt D., Beck M., Schmidt B., Uder M., May M., 2020. Individual calculation of effective dose and risk of malignancy based on Monte Carlo simulations after whole body computed tomography. Scientific Reports. 10(1), 1-12.

14. Akpochafor M.O., Adeneye S.O., Ololade K., Omojola A.D., Adedewe N., Adedokun A., Aweda M., Aboyewa O.B., 2019. Development of computed tomography head and body phantom for organ dosimetry. Iranian Journal of Medical Physics. 16(1), 8-14.

15. Lin H.C., Lai T.J., Tseng H.C., Wang C.H., Tseng Y.L., Chen C.Y., 2019. Radiation doses with various body weights of phantoms in brain 128-slice MDCT examination. Journal of Radiation Research. 60(4), 466-75.

16 .Hsieh C.C., Li C.Z., Lin M.C., Yang Y.J., Hong K.T., Chen Y.H., Syu Z.H., Ju D.T., 2018. Dose comparison using thermoluminescent dosimeters during multislice computed tomography with different parameters for simulated spine tumor examination. Health Physics. 115(2), 275-80.

17. Brady Z., Cain T., Johnston P., 2012. Comparison of organ dosimetry methods and effective dose calculation methods for paediatric CT. Australasian Physical & Engineering Sciences in Medicine. 35(2), 117-34.

18. Osei E.K., Darko J., 2013. A survey of organ equivalent and effective doses from diagnostic radiology procedures. International Scholarly Research Notices. 2013, 1-9.

19. Taha T., Allehyani S., 2020. Measurements Absorbed Doses to Some Organs during Head CT Imaging. International Journal of Science and Research. 9(1), 1-3.

20. Jaffe T.A., Hoang J.K., Yoshizumi T.T., Toncheva G., Lowry C., Ravin C., 2010. Radiation dose for routine clinical adult brain CT: variability on different scanners at one institution. American Journal of Roentgenology. 195(2), 433-8.

21. Brady S.L., Mirro A.E., Moore B.M., Kaufman R.A., 2015. How to appropriately calculate effective dose for CT using either size-specific dose estimates or dose-length product. American Journal of Roentgenology. 204(5), 953-8.

22. Yamashita K., Higashino K., Hayashi H., Takegami K., Hayashi F., Tsuruo Y., Sairyo K., 2021. Direct measurement of radiation exposure dose to individual organs during diagnostic computed tomography examination. Scientific Reports. 11(1), 1-10.

23. Omer H., Alameen S., Mahmoud W.E., Sulieman A., Nasir O., Abolaban F., 2021. Eye lens and thyroid gland radiation exposure for patients undergoing brain computed tomography examination. Saudi Journal of Biological Sciences. 28(1), 342-6.

24. Moore W.H., Bonvento M., Olivieri-Fitt R., 2006. Comparison of MDCT radiation dose: a phantom study. American Journal of Roentgenology. 187(5), 498-502.